Nat. Hazards Earth Syst. Sci., 7, 129–139, 2007
www.nat-hazards-earth-syst-sci.net/7/129/2007/

Natural Hazards and Earth System Sciences

An observational study of the 7 September 2005 Barcelona tornado outbreak

J. Bech[1], R. Pascual[2], T. Rigo[1], N. Pineda[1], J. M. López[2], J. Arús[2], and M. Gayà[3]

[1]Servei Meteorològic de Catalunya, Barcelona, Spain
[2]Instituto Nacional de Meteorología, CMT Catalunya, Barcelona, Spain
[3]Instituto Nacional de Meteorología, CMT Illes Balears, Palma de Mallorca, Spain

Received: 1 November 2006 – Revised: 15 January 2007 – Accepted: 22 January 2007 – Published: 26 January 2007

Abstract. This paper presents an observational study of the tornado outbreak that took place on the 7 September 2005 in the Llobregat delta river, affecting a densely populated and urbanised area and the Barcelona International airport (NE Spain). The site survey confirmed at least five short-lived tornadoes. Four of them were weak (F0, F1) and the other one was significant (F2 on the Fujita scale). They started mostly as waterspouts and moved later inland causing extensive damage estimated in 9 million Euros, three injured people but fortunately no fatalities. Large scale forcing was provided by upper level diffluence and low level warm air advection. Satellite and weather radar images revealed the development of the cells that spawned the waterspouts along a mesoscale convergence line in a highly sheared and relatively low buoyant environment. Further analysis indicated characteristics that could be attributed indistinctively to non-supercell or to mini-supercell thunderstorms.

1 Introduction

Despite the dominant sunny weather and pleasant climate that attracts millions of tourists every season to Spanish Mediterranean beaches, severe weather manifestations occur frequently in summer and autumn over the eastern part of the Iberian Peninsula, particularly on the Mediterranean coastal areas and also the Balearic Islands. Accordingly, in the last decade a number of tornadic cases affecting those areas have been documented in the literature (see for example Martín et al., 1997; Ramis et al., 1997, 1999; Homar et al., 2001, 2003). From a European perspective, a survey by Dotzek (2003) showed the relatively high incidence of tornadoes and waterspouts in Southern Europe Mediterranean coasts. More specifically, a recent 19-year climatology presented by Gayà (2005) indicated that the Spanish regions with higher density of tornadoes were the Balearic Islands and Catalonia (NE Spain, see Fig. 1a), particularly the Barcelona province, recurrently affected by convective heavy rainfall and subsequent flash-flood events (Barrera et al., 2006). As stated by Doswell (2005) the societal impact of severe convective events requires a detailed analysis to improve our understanding of the mechanisms that originate them in order to enhance operational forecast and surveillance capabilities as part of an integrated response.

The purpose of this paper is to present an observational study of the tornado outbreak that took place near Barcelona on the afternoon of 7 September 2005, the event with most tornadoes and waterspouts recorded on one day in Catalonia to date. The four weak and one F2 tornadoes (Fujita, 1981) affected the Barcelona International Airport and other densely populated and urbanised areas causing substantial damage. Air traffic was largely disrupted and the airport was closed for 1 h. Three people were injured but fortunately there were no fatalities. Total losses caused by wind damage were estimated by insurance claims in approximately 9 million Euros.

The tornado outbreak was part of a remarkable longer 4-day convective episode including also heavy rainfall and hail. Two days before (05/09/2005), an intense hailfall produced hen egg sized hailstones in the centre of Catalonia. In those preceding 2 days some observatories registered more than 100 mm of rain, in some cases with high rainfall rates (e.g. 65 mm in 1 h). During the morning of 07/09/2005 precipitation exceeding 100 mm was observed at several observatories in the southern part of Catalonia (near Tarragona, see Fig. 1a) causing some localised urban flooding. The day after the outbreak (08/09/2005) was also rainy so total precipitation amounts collected in those four days (05/09/2005 to 08/09/2005) were generally remarkable with values higher than 100 mm in 11 stations, mostly located in coastal areas. Moreover, that day more funnel clouds and waterspouts were

Correspondence to: J. Bech
(jbech@meteocat.com)

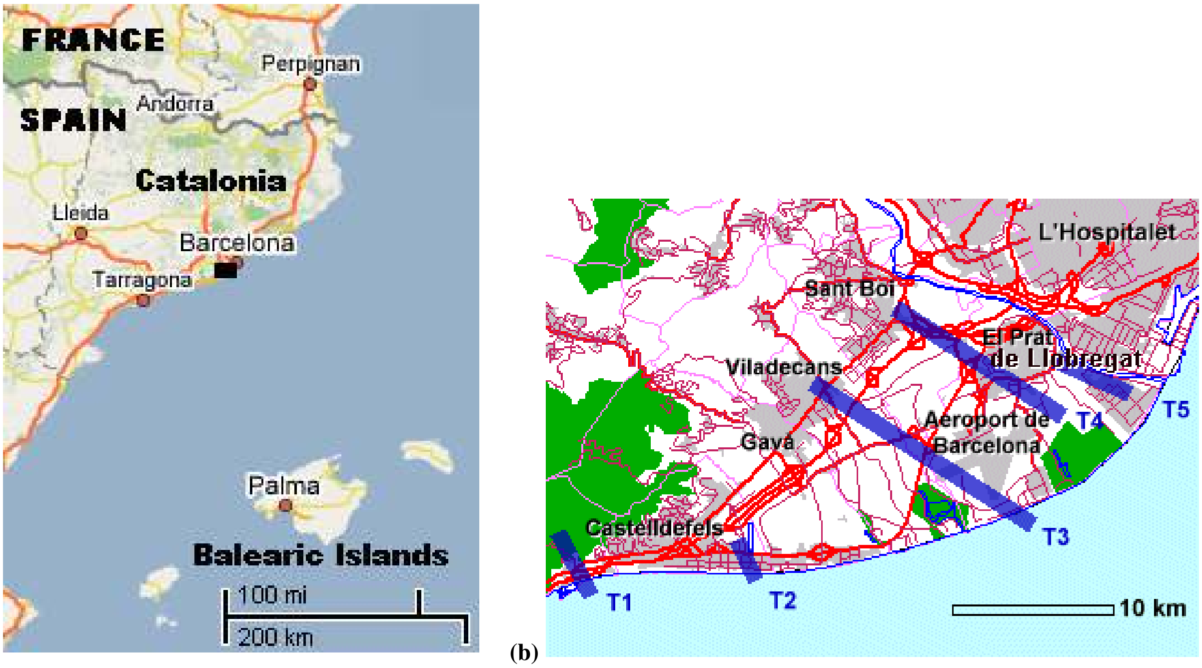

Fig. 1. (a) North-east part of the Iberian Peninsula showing the geographical location of Catalonia and the Balearic Islands; the dark rectangle SW of Barcelona city (Llobregat delta river) is zoomed on the right. **(b)** The Llobregat delta river area showing the approximate location of the five tornado tracks (T1 to T5) revealed by the site survey. Note the Barcelona international airport in El Prat de Llobregat (approximately between T3 and T4).

also observed along the coast of Barcelona and another weak tornado (F1) took place inland (17 km NE of Barcelona city).

The organisation of the paper, which focuses specifically on the tornado outbreak of 07/09/2005, is as follows. Section 2 introduces visual observations of the event and site survey details, Sect. 3 presents a synoptic and mesoscale analysis and Sect. 4 provides a description of remote sensing observations with emphasis on radar data. Section 5 concludes the paper with a discussion of the event.

2 Visual observations and site survey analysis

During the afternoon of 7 September 2005, at least five tornadoes occurred in the SW Barcelona metropolitan area and no less than 10 different funnel clouds could be seen. Though earlier preliminary reports mentioned four distinct tornado tracks approximately parallel (INM, 2005) other eye-witness accounts indicated more than 10 tornadoes, some of them following rather complex trajectories (Massagué, 2005). This apparent contradiction could be explained by the possibility that some well-developed funnel clouds either were only funnel clouds (without an air vortex reaching the ground) or weak tornadoes which left no detectable trace for the post-event site survey and were too distant from the eye-witnesses to verify ground contact (e.g. by flying debris). Another possible explanation is that more than one tornado followed a similar path and they could not be distinguished later in the site survey. The final analysis of the survey and insurance claims allowed confirming five distinct tornado tracks (Fig. 1b). In any case, though it could be considered a small outbreak in terms of US tornado climatology (Galway, 1977), this was the largest outbreak ever recorded in Catalonia, one of the Spanish most tornado-prone regions (Gayà, 2005). In Spain, only a comparable outbreak with six tornadoes that took place in the Balearic Islands in 1996 has been documented previously (Homar et al., 2001).

Most of the vortices started over the sea as waterspouts and moved inland following a south-east to north-west direction finishing their track close to the shoreline probably due to the higher surface friction found inland. Because a great part of the tornado tracks was over urban or suburban areas, the surveying task was started the day after the tornadoes occurred. Evident effects were observed in the towns of Sitges (Fig. 2a), Gavà and El Prat de Llobregat where the Barcelona International Airport is located (Fig. 2b). Moreover, some visual observations indicated the presence of rotational cloud structures (Fig. 2c).

The first tornado started as a waterspout and was observed around 17:00 UTC near the Port Ginesta harbour (in Sitges, SE to Castelldefels). It was rated F1 in the Fujita scale and the path on ground was about 750 m (see Fig. 1b, T1). It damaged a railway power line (see Fig. 2a), two small restaurants,

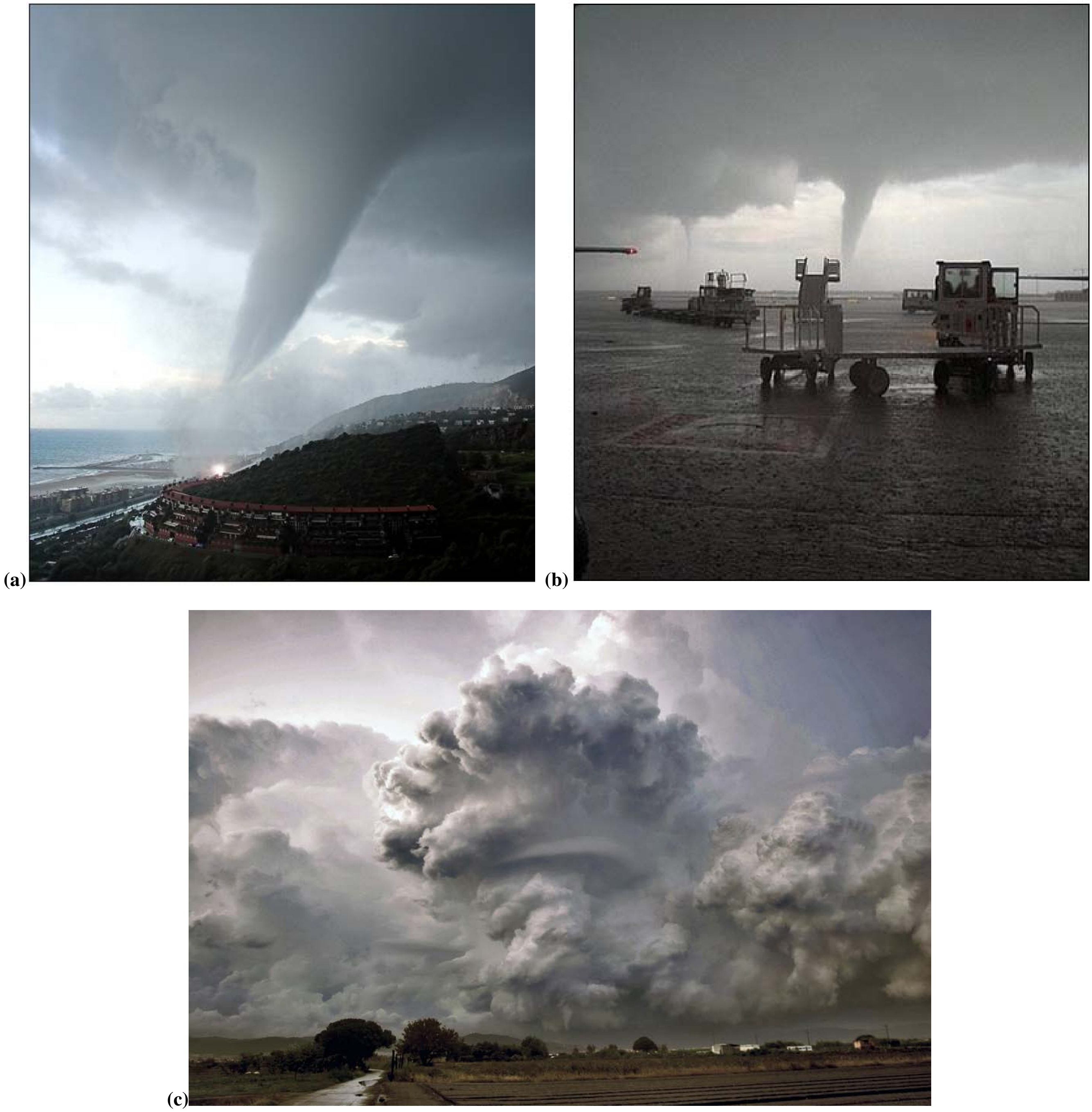

Fig. 2. **(a)** The Port Ginesta tornado (about 17:00 UTC) damaging the railway power lines. **(b)** View from the Barcelona airport runways (17:51 UTC). **(c)** Cloud structures with rotational aspect (18:20 UTC).

several houses, a pine grove and two people were injured. A second shorter track (T2, about 500 m) corresponded to a weaker tornado (F0) that affected the area N of Castelldefels around 17:22 UTC.

The third track (T3) was the longest (7.4 km) and in some parts was 50 m wide. It corresponded to the tornado that crossed the runways of the Barcelona International Airport approximately at 17:50 UTC. The tornado started as a waterspout and was assessed onshore as F1. It then approached the airport and crossed the third runway where it knocked down a Very High Frequency Omnidirectional Range (VOR) radio-navigation antenna and uprooted some signals of the

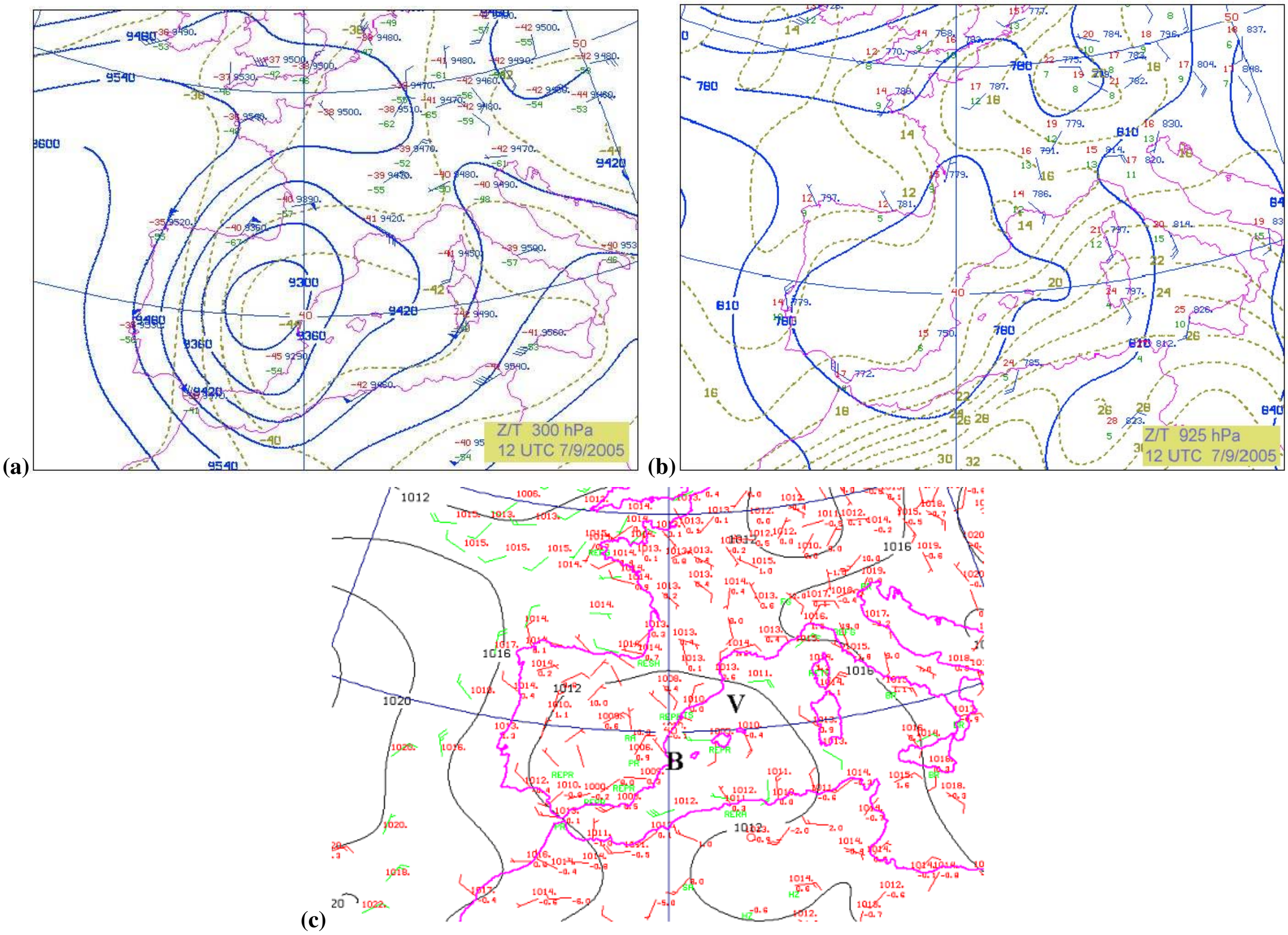

Fig. 3. 7 September 2005, 12:00 UTC ECMWF analysis at 300 hPa **(a)** and 925 hPa **(b)** showing geopotential height (thick line), temperature (dashed line) and synoptic observations and **(c)** surface observations and sea-level pressure analysis indicating the approximate position of the centres of the main (B) and secondary (V) lows.

runways. The vortex increased its force when it was over the platforms and some hangars were destroyed or seriously damaged. Two empty commercial aircraft (a 100-seat jet Fokker 100 and a McDonell Douglas MD-87), were moved or partially lifted and several light ground vehicles (baggage tractors, etc.) were damaged; a small truck was tossed by the wind and the driver was injured. Other aircraft landing or taking off just before the tornadoes experienced strong wind shear but were not directly affected by the tornadoes avoiding more injuries or casualties. The airport was closed to air traffic and was opened after the thunderstorm ended and the runways were cleared of abundant debris. The economic cost of insurance claims in the airport was 1.7 million Euros, excluding the commercial cost of 13 diverted flights, 42 cancellations and 162 delays longer than 1 h.

In spite of these impressive pictures, the survey pointed out that the tornado intensity did not exceed F2. The other two tracks (T4 and T5) were shorter and both corresponded to F0 or weak F1 tornadoes. One of the tracks (T4) was associated with a strong down-flow as indicated by divergent debris found over land when surveying. This seems a clear sign of a microburst that probably accompanied the tornado associated with the T4 track. Microbursts may sometimes generate gustnadoes and occasionally weak tornadoes (Forbes and Wakimoto, 1983) as probably happened in this occasion.

3 Synoptic and mesoscale analysis

In this section the synoptic meteorological framework is examined in order to determine large-scale ingredients and mesoscale factors that favoured the tornadic event. On 6 September 2005 a high-pressure system (1022 hPa) was over Eastern Europe and a cut-off low (with sea-level pressure of 1005 hPa) moved south-eastward over northern Iberian Peninsula (Eden, 2005). The 0.5° grid size ECMWF operational analysis on 7 September at 12:00 UTC indicates that

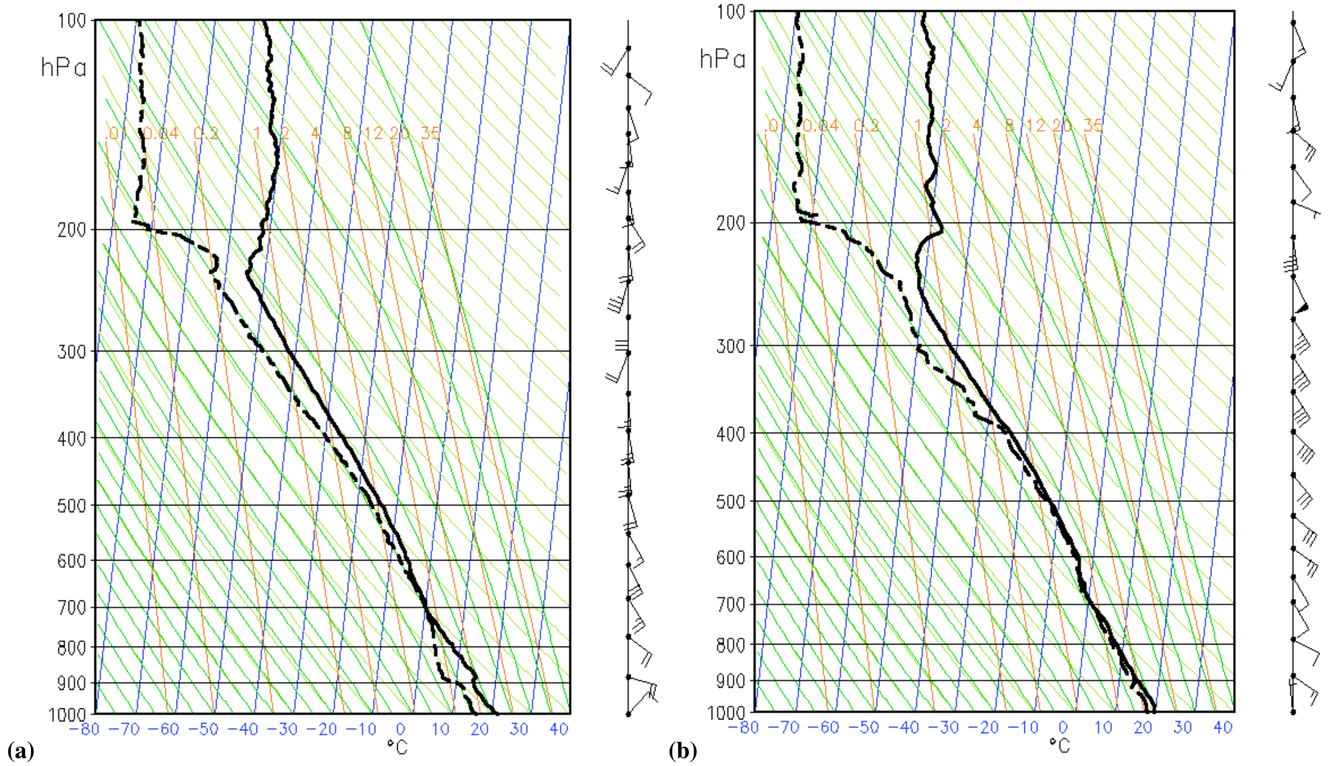

Fig. 4. Stüve diagrams of Barcelona radiosonde observations: **(a)** 07/09/2005 12:00 UTC and **(b)** 08/09/2005 00:00 UTC.

5 h before the outbreak the deep low exhibited a remarkable cold core (−18°C at 500 hPa) and was centred over the north-eastern Iberian Peninsula. A relatively intense northerly jet streak (300 hPa wind speeds greater than 80 kt) was located over the western half of the Iberian Peninsula, in the periphery of the cut-off low (Fig. 3a). During the next 12 h, the low moved south-eastward and the jet streak had a SE-NW orientation. The left part of the jet exit region produced, over central Catalonia, an area of upper-level divergence. As it is well known, when the left exit region of an upper-level jet streak and low-level forcing mechanisms are concurrent then upward vertical motion is favoured and low-level parcels may reach their level of free convection (Carlson, 1991).

The 12:00 UTC synoptic low-level pattern showed a thermal boundary SW-NE oriented over the Western Mediterranean, with the warmer and moister airmass to its SE side, establishing a weak warm air advection below 850 hPa over Catalonia (Fig. 3b). Moreover surface observations (Fig. 3c) and higher resolution analysis based on outputs from INM HIRLAM 0.05° model indicated, between 12:00 and 18:00 UTC, the presence of a low pressure centre below 850 hPa located in front of the Southern Catalonia coast. This configuration established a low-level E/NE flow and a S/SE flow aloft. In the Northern Catalonia coast this low-level flow intensified with time. Model output again indicated a warm air advection with a veering wind profile which was verified in the radar data by an S-shaped zero-isotach radial wind pattern as will be discussed later.

The wind field analysis indicated, below 850 hPa, an E-W oriented convergence line between 12:00 and 18:00 UTC, showing a slow northward displacement. North of the convergence line, the flow was E/NE while at the south side it was from SE to SW. As a consequence, there was horizontal directional shear across the convergence line but no mesoscale temperature gradient was evident.

According to Barcelona radiosonde data, the potential for convective activity diminished notably between 07/09/2005 00 UTC and 12:00 UTC. Stability indices showed then moderate values (for example K-index was 30 K, Total Totals index was 45 K and Lifted Index was −2 K). However they increased in the next 12 h. Surface-based convective available potential energy (CAPE), with virtual temperature correction, evolved from 554 J/kg (07/09/2005 12 UTC) to 669 J/kg (08/09/2005 00:00 UTC). On the other hand, high-level winds (250 hPa) increased with time from 07/09/2005 12:00 UTC (35 kt SW) to 08/09/2005 00:00 UTC (50 kt SE) (Fig. 4) and the easterly low-level wind also intensified and a stronger southeast flow (20 kt) appeared at 850 hPa. The intensity of the low and upper-level jets increased between 12:00 UTC and 17:00 UTC (just before the first tornadoes appeared as shall be seen in the next section). The vertical wind shear value and the storm relative helicity were already

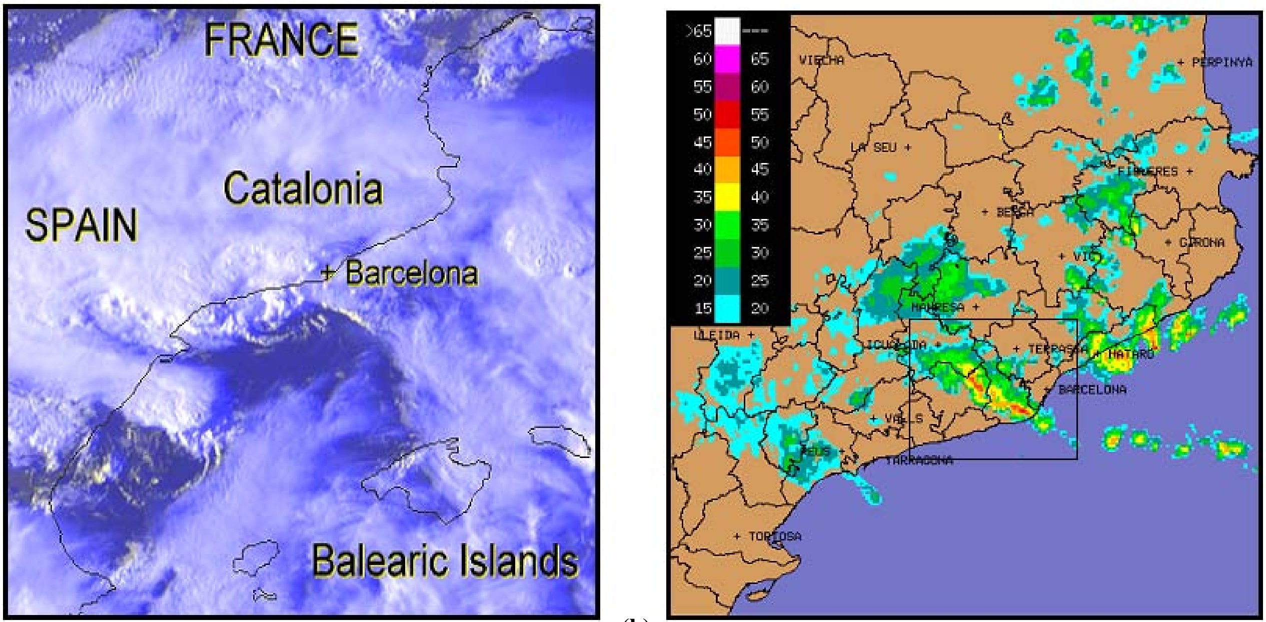

(a) (b)

Fig. 5. (a) MSG HRVIS 16:00 UTC image. **(b)** Radar reflectivity factor (dBZ) 1 km CAPPI 17:38 UTC composite of the SMC radar network; the rectangle indicates the convergence area.

high at 12:00 UTC (0–3 km SRH=247 m^2/s^2). It should be remarked that these values are consistent with the development of intense convective activity associated with severe storms according to previous studies performed in the Western Mediterranean (Tudurí and Ramis, 1997).

4 Remote sensing observations

In this section Meteosat Second Generation (MSG) satellite imagery, radar imagery and lightning observations from the Meteorological Service of Catalonia (SMC) database are used to describe mesoscale features. Lightning information was collected by the Meteocat SAFIR lightning detection system, which uses an interferometric technique in the VHF range (108–116 MHz) to detect total lightning flashes, and a Low Frequency sensor for the detection of Cloud-to-Ground return strokes (Richard and Lojou, 1996). The detection efficiency of the system is between 86 and 92%, according to a field campaign performed in summer 2004 (Montanyà et al., 2006). These values agree with the SAFIR manufacturer specifications (around 90%). The SMC weather radar network is made up by three C-band Doppler systems. The radars acquire polar volumes (radar reflectivity and radial velocity) every six minutes. Further technical details of the SMC weather radars and network characteristics can be found in Bech et al. (2004).

4.1 General description

Convective cells associated with observed waterspouts and tornadoes developed and moved along the convergence line described in the previous section. A cumulus congestus line was observable in MSG-1 high resolution visible channel at 16:00 UTC (Fig. 5a). At 16:40 UTC some small convective cells appeared along the NW-SE oriented line. This spatial distribution of convective cells, developing over the sea (Fig. 5b), and moving NW along the line, persisted until 19:40 UTC. The convective line reached a maximum length of 200 km but the highest radar reflectivity values were located in a shorter part (60 km long) at the western edge of the line. Vertical cross sections along the line showed small intense convective cells over the sea (40–50 dBZ at 4 km) but with low echotops (12 dBZ below 6 km). This vertical reflectivity profile shape is frequently observed in Catalonia maritime areas (Pascual, 2001).

From 16:10 to 20:20 UTC, in the rectangle area marked in Fig. 5b, 504 intra-cloud (IC) and 101 cloud-to-ground (CG) flashes were observed. In the tornadic period (17:00 to 18:00 UTC), there were 92 IC and 17 CG flashes. From the total of 101 CG flashes, only 4 had positive polarity, and no positive CG flashes were registered from 17:00 UTC to 18:00 UTC. The overall IC/CG ratio was 5.0 which corresponds – in terms of severity– to a normal thunderstorm for this region; the 2005 average IC/CG ratio in Catalonia was 5.1 (Pineda, 2006). The temporal evolution of IC and CG flash rate is shown in Fig. 6.

Surface observations, 12:00 UTC Barcelona radiosonde data and Doppler wind field show that an easterly low-level jet (LLJ) was present just north of the convergence line. Maximum velocity (∼110 km/h) was located between 950 m and 1500 m and surface wind gusts reached 100 km/h (17:00 UTC) in some coastal range peaks (500 m a.s.l.). LLJ was observed between 16:04 UTC radar volume scan and 17:08 UTC. Figure 7 shows the intensification of the wind maximum as observed by the Vallirana (PBE) radar. It is important to notice that maximum vertical velocity shear was located over or just north of the horizontal directional shear line. An evolution of the wind profile over the PBE radar is shown in Fig. 8 displaying clearly the vertical wind shear and also the increase in wind speed reaching 50 kt at 1.5 km some 15 min before the onset of the tornado outbreak.

Although at 17:00 UTC the larger dimension of the convective structure was not large enough to be considered a mesoscale convective system (MCS), its shape, internal dynamics and propagation suggest that it could be classified as a back building squall line (Bluestein and Jain, 1985). Furthermore, its very slow movement (∼50 km/3 h) implied that some new convective cells (and new vortices) passed over the same area in the so called convective train effect (Doswell et al., 1996). The squall line was well defined between 16:50 UTC and 18:40 UTC and during this time period some structures resembling mini bow echoes seem to develop along it. At 17:00 UTC, waterspouts were observed in front of Llobregat delta river, associated with new convective cells over the convergence line. Between 17:10 UTC and 18:10 UTC the convective line passed over the Barcelona airport, and surface automated observations showed a wind shift direction (NE changing to SE) and a velocity decrease.

4.2 Other radar smaller scale features

As mentioned above, the radar observed convective structures associated with the waterspouts and tornadoes were relatively low topped and of modest horizontal extension. Classical supercell tornadic storms, characterised by deep convection and the presence of a persistent and intense mid-level mesocyclone – typically 4 to 10 km wide and visible as a characteristic couplet in radar radial wind PPIs – (Doswell and Burgess, 1993) are remarkably different. Non-supercell tornadoes (Wakimoto and Wilson, 1989) lack a mesocyclone and they typically develop misocyclonic rotation along converge lines at low levels. On the other hand, in a different variety of smaller, low-topped supercells known as mini-supercells (McCaul, 1991; Kennedy et al., 1993; Hannesen et al., 1998; Suzuki et al., 2000), the mesocyclone present diameters smaller than 4 km –in fact a misocyclone, in terms of Fujita (1981). From the radar point of view, a number of reasons – including range effects or beam blockage due to complex topography – may hamper mesocyclone and, particularly, misocyclone identification (Chapman et al., 1998; Conejo and Elizaga, 2004). However, in this case the convective structure was relatively near to the PBE radar (located at 620 m ASL); the Barcelona airport is at 20.5 km. Moreover, though there are important blockages to the N (Bech et al., 2003), coverage is good to the S. A velocity couplet was identified in 4 different Plan Position Indicator (PPI) images of the 17:00 UTC PBE volume scan (Fig. 9a). The couplet was embedded in a high vertical shear environment and was located very near the radar (8 km). It extended from 1.5 to 3.0 km and was approximately 2.5 km wide. If associated with a rotating structure, it would be a misoanticyclone. It was observed in the limit of a precipitating structure coming from the SE, the same direction where the tornado shown in Fig. 2a was heading when dissipating. Another remarkable feature, related to the vertical wind shear and the vigorous convective activity, is the overhang structure shown in the relatively low-topped and tilted cell shown in Fig. 9b.

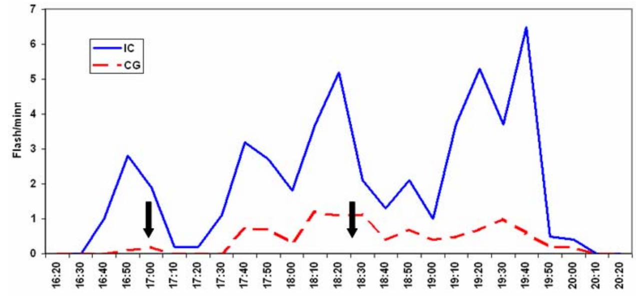

Fig. 6. Time series of intra-cloud (IC) and cloud-to-ground (CG) flash rates in the rectangular area indicated in Fig. 5b. Arrows mark approximately the onset and end of the tornado outbreak.

Figure 10 shows the same cell later (18:34 UTC). The reflectivity structure exhibits a small core with a sharp gradient which resembles the classical "hook echo" shape associated with mesocyclones. The corresponding radial velocity field indicates intense azimuthal shear and might suggest traces of (cyclonic) rotation, though the couplet is not as clear as in Fig. 9a. This cell was coming from the airport and could be associated with the thunderstorm that spawned the F2 tornado.

5 Summary and discussion

An observational description and preliminary diagnostic of the tornadic outbreak of 7 September 2005 in Barcelona is presented. This event, with at least 5 tornadoes, affected the Llobregat delta river, a densely populated area where the Barcelona International Airport is located. The serious hazard that strong convective winds represent to air traffic, particularly for landing and take-off operations, make this event especially relevant.

A possible origin of the general mesoscale setting on 07/09/2005 could be the interaction of the synoptic flow with the Balearic Islands, as suggested by mesoscale lee side vor-

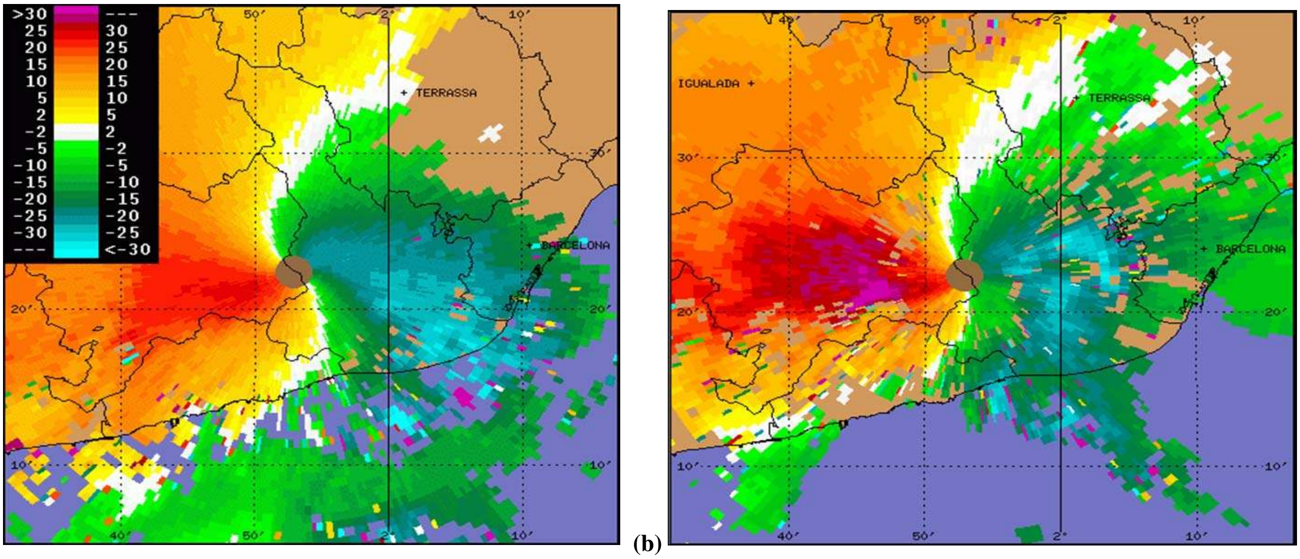

(a) (b)

Fig. 7. 4.0° PPI radial velocity field (m/s) observed by the PBE radar at 16:08 UTC **(a)** and 16:44 UTC **(b)**. The square length is 32 km. Reddish colours denote outbound and greenish colours denote inbound Doppler velocities.

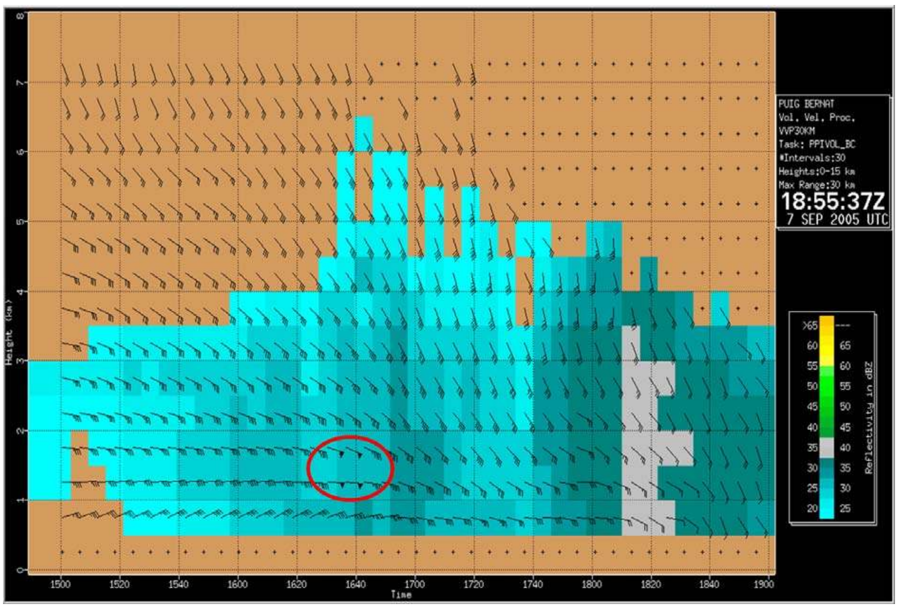

Fig. 8. Velocity Volume Processing (VVP) time series from 15:00 UTC to 19:00 UTC observed by the PBE radar. Z values are on the background. Note the vertical shear and the red circle indicating the wind speed maxima (values up to 50 kt) at 1.5 km prior to the tornado outbreak.

tices present in the wind analysis. In fact, in other strong convective events with a similar synoptic situation, convergence zones with similar characteristics have been identified over the same area (Rigo and Llasat, 2005). In the 07/09/2005 case, the convergence line was forecast by the models a few kilometres northward than suggested by satellite and radar imagery. Homar et al. (2001) identified, in a previous tornadic outbreak near the Balearic Islands, a northward-moving mesoscale convergence line where waterspouts and tornadoes appeared. In the 07/09/2005 case no thermal boundary was diagnosed and a northward-moving mesoscale convergence line was identified. Waterspouts and tornadoes were located on or close to this line in a similar way that was found by Homar et al. (2001). Some au-

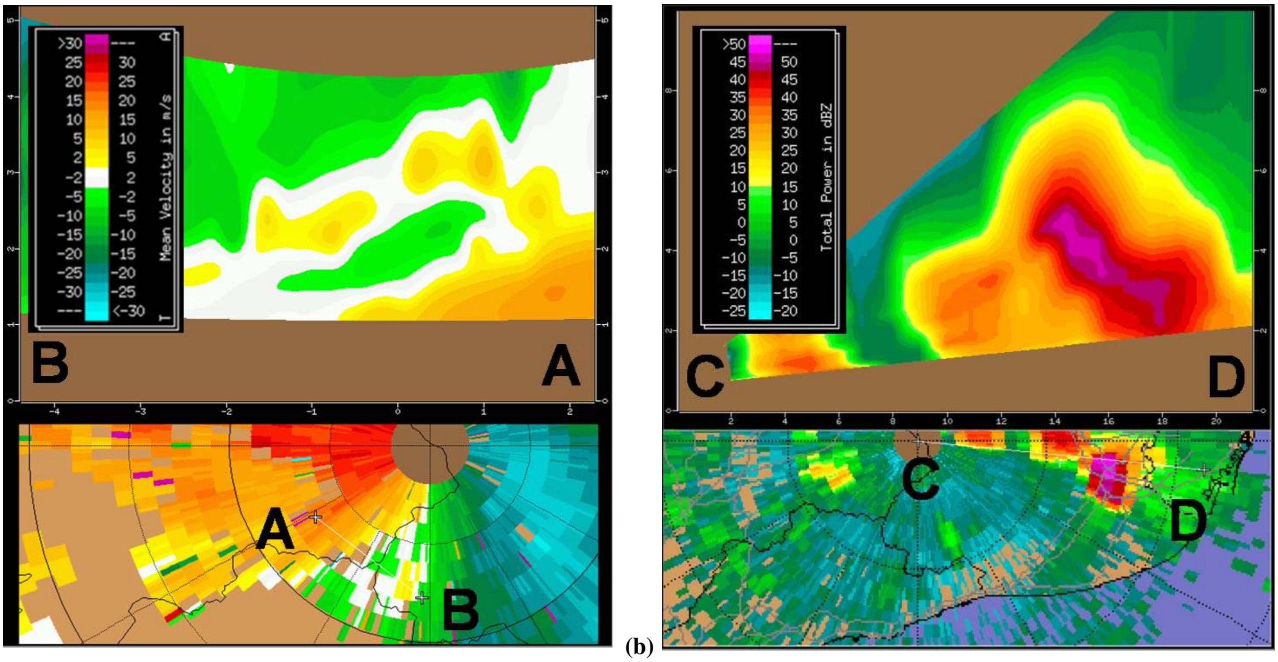

(a) (b)

Fig. 9. (a) PBE radar 6.0° PPI (17:03 UTC) velocity couplet in the radial wind field (bottom) and the corresponding cross section (top) along the segment AB. Rings are at 5 km intervals and maximum height is 5 km. **(b)** PBE radar 16.0° PPI (18:11 UTC) reflectivity factor (bottom) and the corresponding cross section (top) along the segment CD. Rings are at 10 km intervals and maximum height is 10 km.

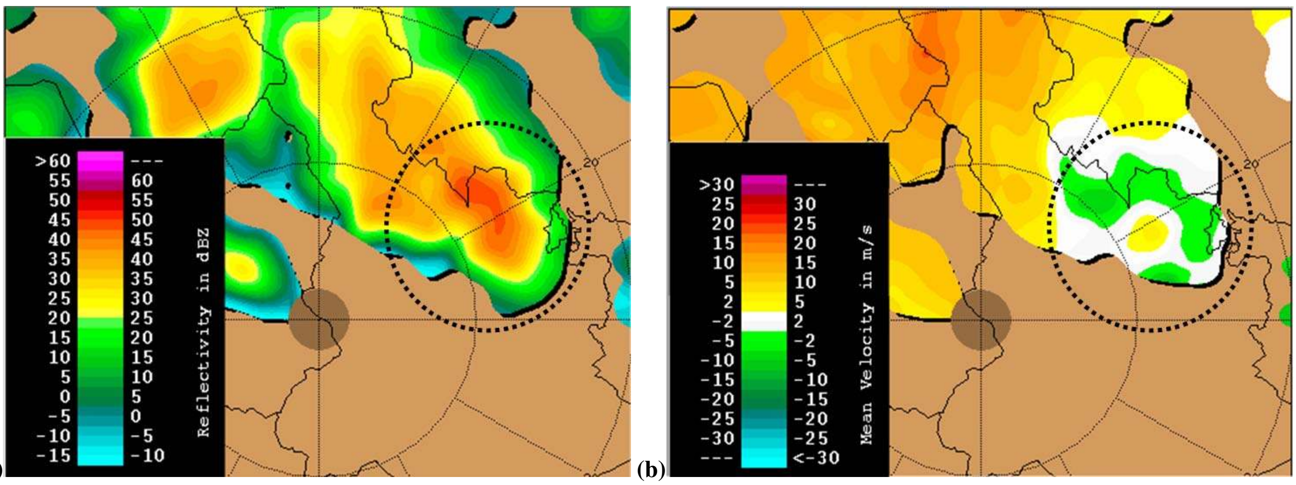

(a) (b)

Fig. 10. PBE radar 8.0° PPI (18:34 UTC): **(a)** reflectivity factor field exhibiting an structure – marked with a dotted circle – similar to a hook echo and **(b)** radial wind field showing a velocity couplet associated with cyclonic rotation. Rings are at 10 km intervals.

thors as Wakimoto and Wilson (1989) or Brady and Szoke (1989) have shown that convergence lines with horizontal wind shear across it are favourable zones to the development of misoscale circulations at lower levels. The presence of a LLJ could contribute to generate cyclonic shear at south side of convergence line and development of Helmholtz instabilities would be possible.

Photographic analysis of waterspouts and tornadoes showed two main characteristics: 1) Funnel clouds connected to cumulus/cumulonimbus bases observed in almost all the cases and 2) Vortices probably developed at the southern edge of the cumulus/cumulonimbus line. Southward of this line cloud development was impeded. The second feature suggests that vortices developed over the shear/convergence line as Wakimoto and Wilson (1989) and Brady and Szoke (1989) proposed to explain non-mesocyclonic (non-supercell) tornadoes. On the other hand, radar observations showed a number of features that might suggest the mini-supercell character of some of the convective structures observed. A possible misoanticyclone could be associated with downdrafts as observed in previous studies of multicell (Kessinger et al., 1988) or supercell storms (Brown and Knupp, 1980; Bluestein et al., 1997; Monteverdi et al., 2001). The strong low-level jet observed and the associated intense vertical shear and horizontal vorticity is a feature compatible both with non-supercell and mini-supercell characteristics of the storms. The intensities of the tornadoes, in case they were of non-supercell origin, would be perfectly in line with Dotzek et al. (2005) who determined that global distribution of tornado intensities is bimodal, in which up to about F2 intensity, the non-mesocyclonic events are more likely. Though the data examined makes clear that the tornadoes were not spawned by classical supercells, it was not possible to discriminate clearly between non-supercell and mini-supercell character of this tornadic outbreak.

Further work could be oriented to examine in more detail the mesoscale and synoptic factors that played a determinant role in the time and location of the tornadogenesis. One possible way could be performing a dual Doppler analysis to retrieve two-dimensional wind fields as done by Alberoni et al. (2000) to analyse the environment of supercell storms in the Po Valley or to apply the test on dynamic and thermodynamic variables related to significant tornadoes suggested by Romero et al. (2006). It should be noted that the coast surrounding the Llobregat delta river area has been affected recurrently by waterspouts or weak tornadoes (<F2). For example, recent observations of waterspouts were made on the 15/11/2005 and 21/02/2006 and another weak tornado was observed on the 13/09/2006 following a similar track to one of the tornadoes of the 07/09/2005 outbreak (i.e. four different events in approximately one year). Therefore it seems plausible that the particular geographical configuration of the delta – flat land entering the sea surrounded by coastal ranges, orientation of the Llobregat river, etc. – might play an important role in such type of events. No doubt the occurrence of a significant (F2) or severe (F3) tornado in the Barcelona urban area –such as the one that hit Madrid in 1886 (Gayà, 2006) – might have devastating effects depending on the precise location and time of the day it took place.

As in previous studies (Martin et al., 1997; Ramis et al., 1997; Homar et al., 2003) it should be remarked, from the operational point of view, that remote sensing observations used here – with the appropriate conceptual models – provide guidance to help forecasters in the surveillance process. However they are of limited use to detect the precise occurrence and location of this type of events and therefore to issue timely warnings to prevent or mitigate their effects.

Acknowledgements. We thank S. Castán by kindly providing extensive insurance information, including the estimated tornado tracks in Fig. 1b. Thanks are also due to AENA, the Spanish aeronautic authority, for detailed data about the wind effects on the Barcelona airport. Pictures shown in Fig. 2 were taken by C. W. Chiu (2a), R. Romero (2b) and M. Massagué (2c), who also provided an extensive report of visual observations. We are also indebted to F. Martín (INM, STAP) for his insightful and encouraging comments during the early stage of this study and to two anonymous reviewers who contributed with constructive criticisms to improve the final form of this paper.

Edited by: U. Ulbrich
Reviewed by: two referees

References

Alberoni, P. P., Levizzani V., Watson, R. J., Holt, A. R., Costa, S., Mezzasalma, P., and Nanni, S.: The 18 June 1997 companion supercells: multiparametric Doppler radar analysis, Meteorol. Atmos. Phys., 75, 101–120, 2000.

Barrera, A., Llasat, M. C., and Barriendos, M.: Estimation of extreme flash flood evolution in Barcelona County from 1351 to 2005, Nat. Hazards Earth Syst. Sci., 6, 505–518, 2006, http://www.nat-hazards-earth-syst-sci.net/6/505/2006/.

Bech, J., Codina, B., Lorente, J., and Bebbington, D.: The sensitivity of single polarization weather radar beam blockage correction to variability in the vertical refractivity gradient, J. Atmos. Oceanic Technol. 20, 845–855, 2003.

Bech, J., Vilaclara, E., Pineda, N., Rigo, T., López, J., O'Hora, F., Lorente, J., Sempere, D., and Fàbregas, F. X.: The weather radar network of the Catalan Meteorological Service: description and applications, Proc. European Radar Conference, 416–420, 2004.

Bluestein, H. B. and Jain, M. H.: Formation of Mesoscales Lines of Precipitation: Severe squall lines in Oklahoma during the spring, J. Atmos. Sci., 42, 1711–1732, 1985.

Bluestein, H. B., Gaddy, S. G., Dowell, D. C., Pazmany, A. L, Galloway., J. C., McIntosh, R. E., and Stein, H.: Doppler Radar Observations of Substorm-Scale Vortices in a Supercell, Mon. Wea. Rev., 125, 1046–1059, 1997.

Brady, R. H., and Szoke, E. J.: A case study of nonmesocyclone tornado development in northeast Colorado: similarities to waterspout formation, Mon. Wea. Rev., 117, 843–856, 1989.

Brown, J. M. and Knupp, K. R.: The Iowa Cyclonic-Anticyclonic Tornado Pair and Its Parent Thunderstorm, Mon. Wea. Rev., 108, 1626–1646, 1980.

Carlson, T. M.: Mid-latitude weather systems, Harper Collins Academic, London, 1991.

Chapman, D., Roberts, N. M., Illingworth, A. J., and Browning, K. A.: First radar detection of a misocyclone in a UK tornadic storm, Weather, 53, 367–368, 1998.

Conejo, S. and Elizaga, F.: Automatic identification of mesocyclones and significative wind structures from Doppler radar data (in Spanish), STAP N.T. 43, 30 pp., INM, Madrid, 2004.

Doswell III, C. A., Brooks, H. E., and Maddox, R. A.: Flash Flood Forecasting: An Ingredients-Based Methodology, Wea. Forecast., 11, 560–581, 1996.

Doswell III, C. A.: Progress toward developing a practical societal response to severe convection (2005 EGU Sergei Soloviev Medal

Lecture), Nat. Hazards Earth Syst. Sci., 5, 691–702, 2005, http://www.nat-hazards-earth-syst-sci.net/5/691/2005/.

Doswell III, C. A. and Burgess, D. W.: Tornadoes and tornadic storms: A review of conceptual models, in: The Tornado: Its Structure, Dynamics, Prediction, and Hazards, edited by: Church, C., Burgess, D., Davies-Jones, B., Doswell, C., American Geophysical Union, Geophysical Monograph 79, Washington DC, 1993.

Dotzek, N., Kurgansky, M. V., Grieser, J., Feuerstein, B., and Névir, P.: Observational evidence for exponential tornado intensity distributions over specific kinetic energy, Geophys. Res. Lett., 32, L24813, doi:10.1029/2005GL024583, 2005.

Dotzek, N.: An updated estimate of tornado occurrence in Europe, Atmos. Res., 67–68, 153–161, 2003.

Eden, P.: Weather Log September 2005, Weather, 60(11), doi:10.1256/wea.224.05, 2005.

Forbes, G. S. and Wakimoto, R. M.: A Concentrated Outbreak of Tornadoes, Downbursts and Microbursts, and Implications Regarding Vortex Classification, Mon. Wea. Rev., 111, 220–236, 1983.

Fujita, T. T.: Tornadoes and downbursts in the context of generalized planetary scales, J. Atmos. Sci., 38, 1511–1534, 1981.

Galway, J. G.: Some climatological aspects of tornado outbreaks, Mon. Wea. Rev., 105, 477–484, 1977.

Gayà, M.: The 1886 tornado of Madrid, Atmos. Res., doi:10.1016/j.atmosres.2005.10.017, in press, 2006.

Gayà, M.: Tornadoes in Spain (1987–2005): temporal and spatial distribution (in Spanish), Rev. Climatol., 5, 9–17, http://webs.ono.com/usr012/reclim/reclim05b.pdf, 2005.

Hannesen, R., Dotzek. N., Gysi, H., and Beheng, K. D.: Case study of a tornado in the Upper Rhine valley, Meteor. Z., N. F. 7, 163–170, 1998.

Homar, V., Gayà, M., and Ramis, C.: A synoptic and mesoscale diagnosis of a tornado outbreak in the Balearic Islands, Atmos. Res., 56, 31–55, 2001.

Homar, V., Gayà, M., Romero, R., Ramis, and C., Alonso, S.: Tornadoes over complex terrain: an analysis of the 28th August 1999 tornadic event in eastern Spain, Atmos. Res., 67–68, 301–317, 2003.

INM: Tornadoes and waterspouts in Catalonia the 7^{th} and 8^{th} of September 2005 (in Spanish), Instituto Nacional de Meteorología. 15 pp., available at: http://www.inm.es/web/sup/ciencia/divulga/tornados_cat/tornados_cat.pdf, 2005.

Kennedy, P. C., Westcott, N. E., and Scott, R. W.: Single-Doppler radar observations of a mini-supercell tornadic thunderstorm, Mon. Wea. Rev., 121, 1860–1870, 1993.

Kessinger, C. J., Parsons, D. B., and Wilson, J. W.: Observations of a storm containing misocyclones, downbursts and horizontal vortex circulations, Mon. Wea. Rev., 116, 1959–1982, 1988.

Martín, F., Riosalido, R., and de Esteban, L.: The Sigüenza tornado: a case study based on convective ingredients concept and conceptual models, Meteorol. Appl., 4, 191–206, 1997.

Massagué, M.: Tornadoes and waterspouts in Barcelona the 7-8 September 2005 (in Catalan), XI J. Meteorol. Eduard Fontserè, ACAM, ISBN 84-934207, 153–162, 2005.

McCaul Jr., E. W.: Buoyancy and shear characteristics of hurricane tornado environments, Mon. Wea. Rev., 119, 1954–1978, 1991.

Montanyà, J., Pineda, N., March, V., Illa, A., Romero, D., and Solà, G.: Experimental evaluation of the Catalan Lightning Location Network, in: 19th Int. Lightning Detection Conf., Tucson, Arizona, USA, 2006.

Monteverdi, J. P., Blier, W., Stumpf, G., Pi, W., and Anderson, K.: First WSR-88D Documentation of an Anticyclonic Supercell with Anticyclonic Tornadoes: The Sunnyvale–Los Altos, California, Tornadoes of 4 May 1998, Mon. Wea. Rev., 4, 207–217, 2001.

Pascual, R.: A radar comparison between severe and efficient thunderstorms in north-east of Iberian Peninsula. 30th International Conference on Radar Meteorology, Munich, American Meteorological Society, 2001.

Pineda, N.: Lightning observations during 2005: the SMC lightning detection network (in Catalan), Servei Meteorològic de Catalunya, http://www.meteo.cat, pp. 8, 2006.

Ramis, C., Arús, J., López, J. M., and Mestres, A. M.: Two cases of severe weather in Catalonia (Spain), An observational study, Meteorol. Applicat., 4, 207–217, 1997.

Ramis, C., López, J. M., and Arús, J.: Two cases of severe weather in Catalonia (Spain), A diagnostic study, Meteorol. Applicat., 6, 11–27, 1999.

Richard, P. and Lojou, J. Y.: Assessment of application of storm cell electrical activity monitoring to intense precipitation forecast, in: 10th Int. Conf. on Atmospheric Electricity, Osaka, Japan, pp. 284–287, 1996.

Rigo, T. and Llasat, M. C.: Radar analysis of the life cycle of Mesoscale Convective Systems during the 10 June 2000 event, Nat. Hazards Earth Syst. Sci., 5, 959–970, 2005, http://www.nat-hazards-earth-syst-sci.net/5/959/2005/.

Romero, R., Gayà, M., and Doswell III, C. A.: European climatology of severe convective storm environmental parameters: A test for significant tornado events, Atmos. Res., doi:10.1016/j.atmosres.2005.06.011, in press, 2006.

Suzuki, O., Niino, H., Ohno, H., and Nirasawa, H.: Tornado-Producing Mini Supercells Associated with Typhoon 9019, Mon. Wea. Rev., 128, 1868–1882, 2000.

Tudurí, E. and Ramis, C.: The environment of significant convective events in the Western Mediterranean, Wea. Forecast., 12, 294–306, 1997.

Wakimoto, R. M. and Wilson, J. W.: Non-supercell tornadoes, Mon. Wea. Rev., 117, 1113–1140, 1989.